Chinese Chemical Letters 31 (2020) 455–458

Contents lists available at ScienceDirect

Chinese Chemical Letters

journal homepage: www.elsevier.com/locate/cclet

Communication

A fast and colorimetric sensor array for the discrimination of ribonucleotides in human urine samples by gold nanorods

Dan Yuan, Huihong Yan, Jiahui Liu, Jiajun Liu, Chunmei Li, Jian Wang*

Key Laboratory of Luminescent and Real-Time Analytical Chemistry (Southwest University), Ministry of Education, College of Pharmaceutical Sciences, Southwest University, Chongqing 400715, China

ARTICLE INFO

Article history:
Received 16 June 2019
Received in revised form 29 July 2019
Accepted 31 July 2019
Available online 1 August 2019

Keywords:
Gold
Nanorods
Ribonucleotides
Chemical etching
Principal component analysis
Sensor array

ABSTRACT

Ribonucleotides are usually functioned as biomarkers to diagnose diseases and monitor the life activities in living organisms, and their discrimination is of great significance but challenging. Taking advantage of the unique characteristics of gold nanorods (AuNRs), herein, a colorimetric sensor array for discrimination of twelve ribonucleotides was developed based on the chemical etching of AuNRs with controllable aspect ratios. During the etching process, AuNRs were preferentially shortened and eventually turned into Au(III) state by Fenton's reaction. The morphological change of AuNRs led to the significant color change and blue shift in the corresponding extinction spectrum. However, when Fe^{2+} bound with ribonucleotides, the Fenton's reaction was prevented and the ability to etch AuNRs was weakened or disappeared. Due to the different structures of nucleotides, the binding ability of them with Fe^{2+} was distinct, resulting in the discrepancy in the chemical etching of AuNRs, which could be developed for distinguishing ribonucleotides. Moreover, the proposed sensor array was successfully explored to distinguish ribonucleotides in complex human urine samples.

Ribonucleotides species are one linchpin in biological field, which play vital roles in physiological processes such as energy supply, metabolism, and transmission of genetic information in organisms [1]. For example, guanosine triphosphate (GTP) is involved in the synthesis of RNA, DNA proteins and intracellular nutrient metabolism [2,3]. Adenosine diphosphate (ADP) plays an important role in the fundamental biological reactions catalyzed by adenosine triphosphatase (ATPases) and kinases [4]. Moreover, these small biomolecules often functioned as biomarkers to diagnose diseases and monitor the life activities in living organisms. Therefore, sensors for physiological ribonucleotides are of vital importance for investigating the metabolic processes and diseases diagnosis. With this issue in mind, great efforts have been devoted to developing sensitive and selective methods for ribonucleotide detection in the past decades, including fluorometry [5–7], spectrophotometry [8], nuclear magnetic resonance spectroscopy [9], chromatography [10], electrochemical analysis [11,12], and aptamer-based optical sensing [13], and so on. These methods can only selectively detect one kind of ribonucleotide and/or require sophisticated instrumentation, and just few attempts have been reported for distinguishing twelve ribonucleotides at the same time. Accordingly, the development of simple, rapid, and novel strategies for large-scale determination of ribonucleotides is highly desirable.

The array sensing and colorimetric methods have been receiving considerable attention [14]. By now, a large number of sensor arrays have been proposed to detect and distinguish some similar biomolecules, such as metal ions [15–17], bacteria [18], phosphate [19,20] and proteins [21–25]. Despite the progress, further developments in the pattern-based assay for large-scale applications are hampered by limitations with respect to some complex or expensive operations, such as high-cost and complicated synthesis and the difficult design of pattern recognition elements. Therefore, developing usable and cost-effective but versatile pattern recognition elements is indispensable for the development of "chemical nose/tongue" with excellent discrimination capabilities.

With the development of nanotechnology, noble metals nanomaterial attracted considerable attention [26]. As a one-dimensional nanomaterial with unique optical properties, gold nanords (AuNRs) present two attractive and independent transverse and longitudinal localized surface plasmon resonances (LSPR) bands, which correspond to the transverse and longitudinal electronic vibration [27], respectively. Especially, the longitudinal plasmon resonance absorption (LPRA) is closely related with the aspect ratio [28], which show a variety of colors and promising applications in

* Corresponding author.
E-mail address: wj123456@swu.edu.cn (J. Wang).

https://doi.org/10.1016/j.cclet.2019.07.067
1001-8417/

the visual assays. Numerous investigations have reported that the aspect ratios of AuNRs can be adjusted by H_2O_2, I^-, Fe^{3+} and other oxidizing substances (such as ·OH), which are accompanied by the significant color diversification and thus enable the visual sensing [29,30]. Therefore, this property makes AuNRs possible to act as an ideal probe for colorimetric detection. In addition, it is well known that under acidic conditions, Fe^{2+} can act as a catalyst to disproportion H_2O_2, thereby yielding two different kinds of oxygen-radical species of ·OH and ·OOH, which is called Fenton's reaction [31]. On the one hand, in the Fenton's reaction, Fe^{2+} reacts with H_2O_2 to form Fe^{3+} and ·OH, and the oxidizability of ·OH is much stronger than H_2O_2. On the other hand, the formed Fe^{3+} also can react with H_2O_2 to form Fe^{2+} and ·OOH, resulting in the Fenton's reaction to accelerate the oxidation rate [32], which could be utilized to adjust the aspect ratio of AuNRs to realize the visual detection of biomolecules [33–35].

Inspired by the above facts, we herein for the first time demonstrate a novel, fast and multichannel colorimetric sensor array for identifying and detecting twelve ribonucleotides (Scheme 1). Firstly, AuNRs with four different aspect ratios were introduced as sensor arrays, which changed from rod-shape to spheres in morphology and blue-shift of LPRA after etched by ·OH. Then, in the presence of nucleotides that contain phosphoric acid and base, Fe^{2+} could bind with ribonucleotides to prevent H_2O_2 from yielding ·OH. Because of the unequal affinity of different ribonucleotides with Fe^{2+}, it produces certain diversity during the etching process of AuNRs to realize the distinguishing of twelve ribonucleotides. In comparison with previous reports [36], this colorimetric method, which was based on the LPRA shift of AuNRs, was much faster and simpler. Furthermore, it not only could avoid the difficult surface modification procedures and chromogenic reagents, but also distinguish ribonucleotides in human urine samples.

According to the previously reported seed-mediated method [37], AuNRs with four different aspect ratios were prepared by adjusting the amount of reagents in the synthesis process. The LPRA bands located at 693 nm, 722 nm, 744 nm, and 902 nm (Fig. S1a in Supporting information) and the corresponding aspect ratios of AuNRs were 2.3, 2.9, 3.1 and 4.5, respectively (Fig. S1b in Supporting information). The SEM images of etched AuNRs (Fig. 1a) displayed that in the presence of H_2O_2 and Fe^{2+}, the morphology of AuNRs changed from rod-shape to sphere. After introducing ATP, the morphology of AuNRs restored to a rod shape, indicating that ATP can bind with Fe^{2+} and hinder the etching process of AuNRs.

Under the Fenton's reaction conditions, the LPRA of AuNRs underwent a significant blue shift in absorption spectra, and the peak positions were all blue-shifted to about 550 nm (Fig. 1b), indicating that the morphology of AuNRs changed from rod-shape to sphere. After introducing different ribonucleotides, the LRPA of AuNRs underwent distinct degrees of red shift compared with AuNRs etched by the Fenton's reaction, indicating that ribonucleotides could bind with Fe^{2+}, thereby inhibiting the generation of ·OH in the Fenton's reaction and hindering the etching of AuNRs. The difference in binding ability between various ribonucleotides and Fe^{2+} led to different red shift of LPRA. From the spectral shift, the following conclusions can be drawn that GTP has the strongest binding ability with Fe^{2+}, followed by UTP > ATP > CTP, inferring that when the number of phosphate groups is the same, the binding ability of the four kinds of bases with Fe^{2+} can be arranged in the order of guanine > uracil > adenine > cytosine. This phenomenon may be attributed to that the N atoms on the anthracene ring, or the pyrimidine ring, or the amino group, have a lone pair of electrons, which can bind with Fe^{2+}. At the same time, the guanine and uracil structures with carbonyl groups are capable of forming metal carbonyl complexes with metal ions, which may result in strong binding affinity of guanine and uracil with Fe^{2+}.

In order to obtain the greatest distinguishing performance, discrimination conditions were further optimized. Three critical factors, including the concentrations of Fe^{2+}, H_2O_2 and HCl in the Fenton's reaction, were taken into consideration. When the concentrations of Fe^{2+} and H_2O_2 were at very low levels, the yield of ·OH was insufficient and AuNRs cannot be completely etched. When Fe^{2+} and H_2O_2 were excessive, many other reactions are also possible, which include the radical-radical reaction or the reaction of the ·OH radical with H_2O_2 [38], greatly reducing the utilization of ·OH and the rate of etching AuNRs. When the concentrations of Fe^{2+} and H_2O_2 were 180 μmol/L and 0.26 mmol/L (Figs. S2a and S2b in Supporting information), it was ideal for discrimination. Simultaneously, since the Fenton's reaction can only occur in acidic solution, thus, the concentrations of HCl was investigated. At high pH (pH > 4), the generation of ·OH became slower because of the formation of the ferric hydroxo complexes. On the other hand, in strongly acidic medium (pH < 2.0), the reaction was decelerated due to the formation of complex species $[Fe(H_2O)_6]^{2+}$ [38], which influenced the balance between the Fe^{2+} and Fe^{3+}. Therefore, about 85 mmol/L HCl was observed to obtain nearly the maximum shift of absorption (Δλ, Fig. S2c in Supporting information).

Under the optimal conditions, twelve ribonucleotides were distinguished by the multichannel colorimetric sensor array at the concentrations of 100 μmol/L, 250 μmol/L, and 500 μmol/L, respectively. The colourful photos (Fig. S3a in Supporting information) for distinguishing twelve ribonucleotides at 100 μmol/L show that besides the three pairs ribonucleotides (CMP and UMP, CDP and UDP, CTP and GTP), others can be recognized by the naked eye. To further evaluate the discriminative capability of this sensing array, PCA was also performed to provide further evidence for the array's recognition capability for ribonucleotides (Fig. S3c in Supporting information), which shows that only one pair of ribonucleotides (CDP and UDP) cannot be distinguished.

Next, twelve ribonucleotides at concentration of 250 μmol/L was taken into consideration (Fig. 2). The result indicated that the colorimetric arrays of three ribonucleotides (CMP, CDP, and UDP) were similar. When PCA was performed, the PCA score map supported the conclusion that twelve ribonucleotides could be clearly distinguished. Finally, if twelve ribonucleotides were distinguished at a higher concentration of 500 μmol/L (Fig. S4 in Supporting information), they could be more easily distinguished by the colourful photos and PCA score. From the above results, it can be drawn the conclusion that when the concentration of ribonucleotides were 100 μmol/L, CDP and UDP cannot be distinguished. However, when the concentrations were greater than 100 μmol/L, various ribonucleotides can be clearly distinguished by PCA score. Simultaneously exploiting the data processing method of PCA, the distinguishing ability of this multi-channel array can be improved.

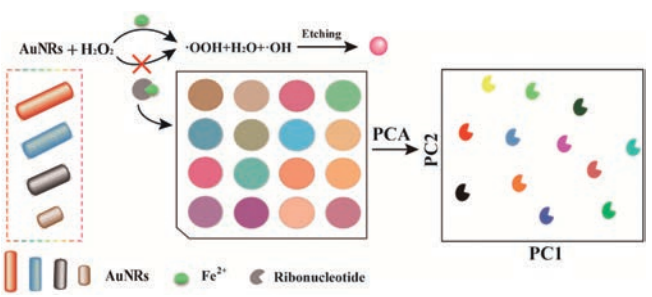

Scheme 1. AuNRs with four aspect ratios as probes for distinguishing twelve ribonucleotides.

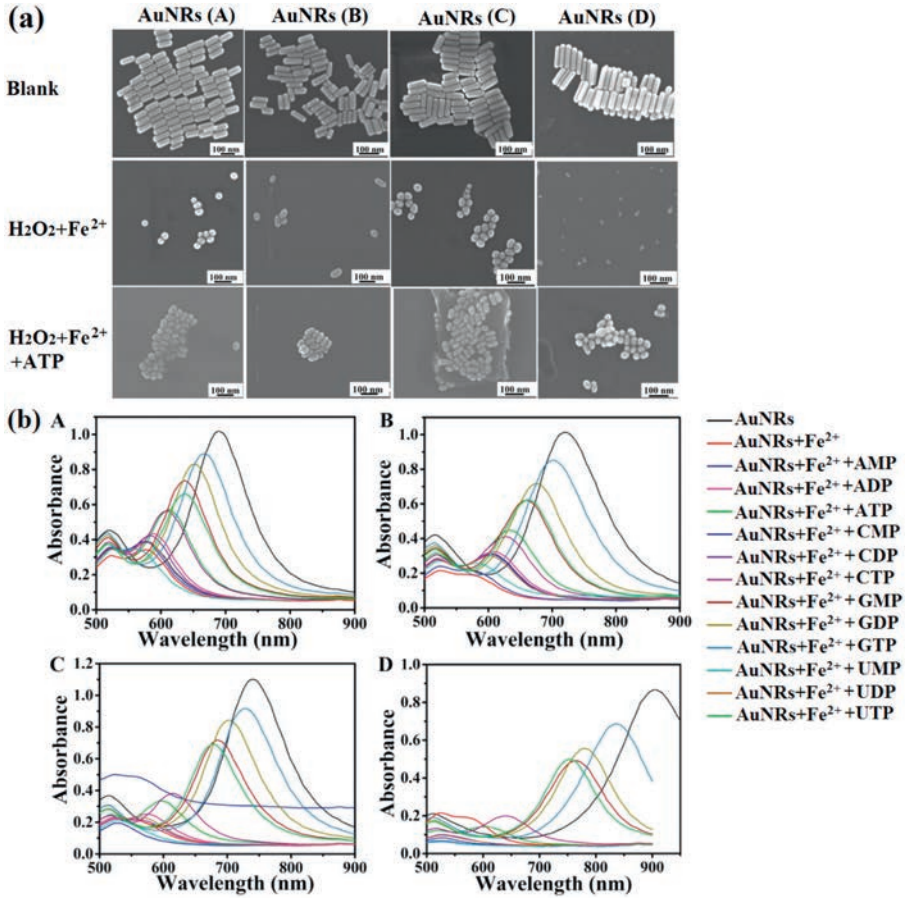

Fig. 1. The etching features of AuNRs. (a) SEM images of AuNRs with controllable aspect ratios under different conditions. Conditions: [H_2O_2], 0.26 mmol/L; [Fe^{2+}], 0.18 mmol/L; [ATP], 500 μmol/L; [HCl], 85 mmol/L. Scale bar: 100 nm. (b) The UV–vis absorption spectra of AuNRs with four aspect ratios etched by Fe^{2+} and H_2O_2 in the presence of different ribonucleotides: AuNRs (A), AuNRs (B), AuNRs (C), AuNRs (D). Conditions: [H_2O_2], 0.26 mmol/L; [Fe^{2+}], 0.18 mmol/L; [ribonucleotides], 250 μmol/L; [HCl], 85 mmol/L.

To evaluate the reliability and accuracy of the sensor array, eleven unknown samples were randomly selected and performed according to the colorimetric sensor array. After adding the ribonucleotides to the samples, the absorption spectra of AuNRs were collected and then analyzed by PCA. PC1 and PC2 of unknown samples were compared with the PCA score map (Fig. 2c). The results (Table S2 in Supporting information) indicate that the eleven unknown samples were correctly identified with an identification accuracy of 100%, indicative of the feasibility of using this sensor array in identifying unknown ribonucleotides.

To guarantee the feasibility of the proposed sensor array in accessible biofluids, urine samples were collected from healthy people, and added the following ribonucleotides and their mixtures to the urine sample, ADP, ATP, CTP, GMP, GTP, ATP + ADP (molar ratios = 1:1), ATP + ADP (molar ratios = 3:1). The results of PCA plots (Fig. 3) indicate that urine samples without

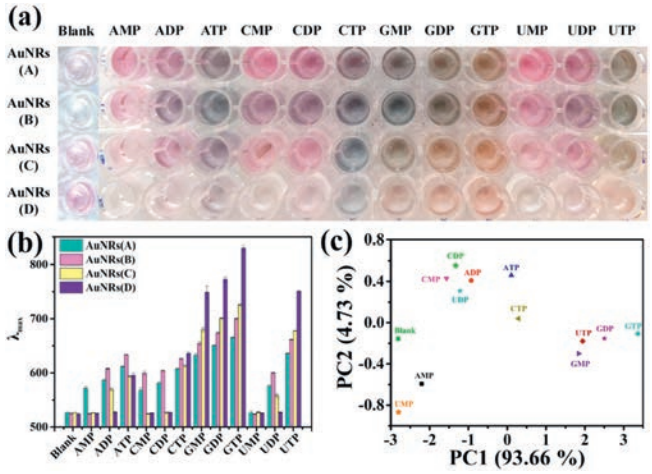

Fig. 2. The distinguishing of twelve ribonucleotides at 250 μmol/L. (a) The visual photos of AuNRs induced by twelve nucleotides; (b) and (c) are the fingerprints (response patterns) of various ribonucleotides generated by AuNRs sensor array and canonical score plot for the response patterns as obtained from PCA. Conditions: [H_2O_2], 0.26 mmol/L; [Fe^{2+}], 0.18 mmol/L; [ribonucleotides], 250 μmol/L; [HCl], 85 mmol/L.

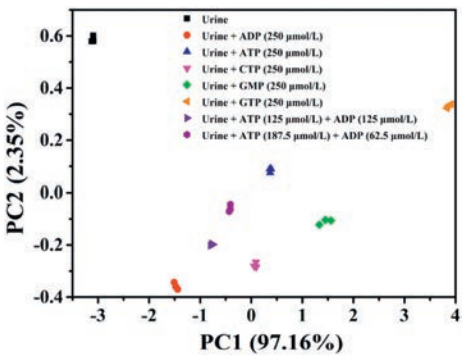

Fig. 3. The distinguishing of nucleotide in urine samples. Conditions: [H_2O_2], 0.26 mmol/L; [Fe^{2+}], 0.18 mmol/L; [ribonucleotides], 250 μmol/L; [HCl], 85 mmol/L.

ribonucleotides produce their own unique signals, while urine samples containing different ribonucleotides showed unique PCA signals. At the same time, it was found that the mixtures samples also had unique PCA signals, and the regions did not overlap, indicating that the method can be used to distinguish the ribonucleotides in urine samples.

In summary, a multichannel AuNRs sensor array for differentiation analysis of ribonucleotides was developed based on the etching of AuNRs. Firstly, the sensor array exhibited the advantage of low cost, time saving, and simplicity. At the same time, four different aspect ratio AuNRs were used as multichannel sensing probes to realize the distinguishing of ribonucleotides and their mixtures in urine samples. Secondly, the proposed sensor array was successfully explored the binding ability between ribonucleotides and Fe^{2+} and the following conclusion had been summarized: when the number of phosphate groups was equal in ribonucleotides, the binding ability of the four kinds of bases with Fe^{2+} can be arranged in the order of guanine > uracil > adenine > cytosine. This conclusion may provide a basis for studying the binding ability between ribonucleotides and other metal ions. Finally, it is believed that different aspect ratio of AuNRs that can be used as sensor array probes may provide new opportunities for the development of multichannel sensing platforms, as well as the construction of multi-sensor components.

Acknowledgments

All authors are grateful to the Natural Science Foundation Project of China (No. 21405123) and Fundamental Research Funds for the Central Universities (No. XDJK2019AC002) for the financial support. Additionally, we appreciate the valuable suggestions of Professor Fengyu Li from Jinan University.

Appendix A. Supplementary data

Supplementary material related to this article can be found, in the online version, at doi:https://doi.org/10.1016/j.cclet.2019.07.067.

References

[1] D.C. Hargreaves, G.R. Crabtree, Cell Res. 21 (2011) 396–420.
[2] M. Moosavi, R. Yazdanparast, A. Lotfi, J. Biochem. Mol. Bio. 39 (2006) 492–501.
[3] G.F. von Mollard, T.C. Südhof, R. Jahn, Nature 349 (1991) 79–81.
[4] D.D. Hackney, ACS Chem. Bio. 5 (2010) 353–354.
[5] J.M. Bai, L. Zhang, R.P. Liang, J.D. Qiu, Chem.-Eur. J. 19 (2013) 3822–3826.
[6] Y. Wu, J. Wen, H. Li, S. Sun, Y. Xu, Chin. Chem. Lett. 28 (2017) 1916–1924.
[7] M. Zhang, S.M. Guo, Y.R. Li, P. Zuo, B.C. Ye, Chem. Commun. (Camb.) 48 (2012) 5488–5490.
[8] C.M. Li, Y.F. Li, J. Wang, C.Z. Huang, Talanta 81 (2010) 1339–1345.
[9] N.A. Esipenko, P. Koutnik, T. Minami, L. Mosca, V.M. Lynch, et al., Chem. Sci. 4 (2013) 3617–3623.
[10] J.B. Quintana, R. Rodil, T. Reemtsma, Anal. Chem. 78 (2006) 1644–1650.
[11] K. Zhang, X. Zhu, J. Wang, L. Xu, G. Li, Anal. Chem. 82 (2010) 3207–3211.
[12] W.L. Cheng, J.W. Sue, W.C. Chen, J.L. Chang, J.M. Zen, Anal. Chem. 82 (2010) 1157–1161.
[13] M. Wang, J. Chen, D. Su, G. Wang, X. Su, Talanta 198 (2019) 1–7.
[14] Y. Huang, J. Chen, S. Zhao, et al., Anal. Chem. 85 (2013) 4423–4430.
[15] G. Sener, L. Uzun, A. Denizli, ACS Appl. Mater. Inter. 6 (2014) 18395–18400.
[16] W. He, L. Luo, Q. Liu, Z. Chen, Anal. Chem. 90 (2018) 4770–4775.
[17] Z. Long, D.C. Fang, H. Ren, J. Ouyang, L. He, et al., Anal. Chem. 88 (2016) 7660–7666.
[18] B. Li, X. Li, Y. Dong, B. Wang, D. Li, et al., Anal. Chem. 89 (2017) 10639–10643.
[19] S. Sun, K. Jiang, S. Qian, Y. Wang, H. Lin, Anal. Chem. 89 (2017) 5542–5548.
[20] H. He, C. Li, Y. Tian, P. Wu, X. Hou, Anal. Chem. 88 (2016) 5892–5897.
[21] H. Xi, W. He, Q. Liu, Z. Chen, ACS Sustain. Chem. Eng. 6 (2018) 10751–10757.
[22] X. Wei, Y. Wang, Y. Zhao, Z. Chen, Biosens. Bioelectron. 97 (2017) 332–337.
[23] S. Xu, Y. Wu, X. Sun, Z. Wang, X. Luo, J. Mater. Chem. B Mater. Biol. Med. 5 (2017) 4207–4213.
[24] H. Kong, D. Liu, S. Zhang, X. Zhang, Anal. Chem. 83 (2011) 1867–1870.
[25] M. Sun, L. Wu, H. Ren, X. Chen, J. Ouyang, et al., Anal. Chem. 89 (2017) 11183–11188.
[26] M. Li, J. Chen, J. Pan, Z. Huang, H. Qiu, Chin. Chem. Lett. 30 (2019) 541–544.
[27] J. Pérez-Juste, I. Pastoriza-Santos, L.M. Liz-Marzán, P. Mulvaney, Coord. Chem. Rev. 249 (2005) 1870–1901.
[28] S. Link, M.B. Mohamed, M.A. El-Sayed, J. Phys. Chem. B 103 (1999) 3073–3077.
[29] X. Ma, Z. Chen, P. Kannan, et al., Anal. Chem. 88 (2016) 3227–3234.
[30] Z. Zhang, Z. Chen, S. Wang, F. Cheng, L. Chen, ACS Appl. Mater. Inter. 7 (2015) 27639–27645.
[31] J. Liu, C. Dong, Y. Deng, et al., Water Res. 145 (2018) 312–320.
[32] Y.W. Kang, K.Y. Hwang, Water Res. 34 (2000) 2786–2790.
[33] H. Yang, A. Liu, M. Wei, et al., Anal. Chem. 89 (2017) 12094–12100.
[34] X. Ma, Z. Chen, P. Kannan, et al., Anal. Chem. 88 (2016) 3227–3234.
[35] Z. Zhang, Z. Chen, F. Cheng, Y. Zhang, L. Chen, Biosens. Bioelectron. 89 (2017) 932–936.
[36] G.V. Zyryanov, M.A. Palacios, P. Anzenbacher Jr., Angew. Chem. Int. Ed. 46 (2007) 7849–7852.
[37] X. Ye, C. Zheng, J. Chen, Y. Gao, C.B. Murray, Nano Lett. 13 (2013) 765–771.
[38] İ. Gulkaya, G.A. Surucu, F.B. Dilek, J. Hazard. Mater. 136 (2006) 763–769.